ISSN 0036-0244, Russian Journal of Physical Chemistry A, 2020, Vol. 94, No. 13, pp. 2784–2796. © Pleiades Publishing, Ltd., 2020.

STRUCTURE OF MATTER AND QUANTUM CHEMISTRY

Conformational, Structural, Vibrational, Electronic, and Molecular Docking Studies of 3-Formylphenylboronic Acid and 4-Formylphenylboronic Acid: A Comparative Study

E. Tanış[a,*], M. Kurt[b], Serap Yalçın[c], and Fahriye Ercan[d]

[a] *Department of Electrical and Electronics Engineering, Kırşehir Ahi Evran University, Kırşehir, Turkey*

[b] *Department of Biophysics, Kırşehir Ahi Evran University, Kırşehir, Turkey*

[c] *Department of Molecular Biology and Genetic, Kırşehir Ahi Evran University, Kırşehir, Turkey*

[d] *Department of Plant Protection, Kırşehir Ahi Evran University, Kırşehir, Turkey*

** e-mail: eminetanis@ahievran.edu.tr*

Received January 8, 2020; revised February 10, 2020; accepted March 11, 2020

Abstract—Phenylboronic acids are used as synthetic intermediates in organic synthesis Suzuki-Miyaura reaction is important for the synthesis of many inhibitors of serine proteases. Geometry optimization was performed for the eight possible conformations of 3-formylphenylboronic acid (3FPBA) and 4-formylphenylboronic acid (4FPBA) using the DFT/B3LYP method with the 6-311++G(*d*,*p*) basis set. According to the theoretical calculation results, C3 conformation was found more stable than other conformations. The compounds 3FPBA and 4FPBA were investigated by using FT-IR (4000–400 cm^{-1}), dispersive Raman (4000–40 cm^{-1}) spectroscopy and theoretical DFT/B3LYP/6-311++G(*d*,*p*) calculations. The calculation results have been compared with observed values, which agree with each other. Natural bonding orbital (NBO) analysis was performed to analyze the hyper-conjugative stability of the molecule, molecular orbital interaction and charge delocalization. Frontier orbitals (FMOs) were identified to describe the reactivity of the title molecules. The calculated UV–Vis absorption spectrum was analyzed using the TD-DFT approach. Furthermore, molecular docking studies of 3FPBA and 4FPBA compounds were performed with anti-apoptotic proteins. Our finding shows compounds 3FPBA and 4FPBA have same binding affinity with each of anti-apoptotic proteins.

Keywords: phenylboronic acid, DFT, frontier orbital analysis, MEP, docking

DOI: 10.1134/S0036024420130282

1. INTRODUCTİON

Boronic acid derivatives are highly demanded reagents [1, 2]. Boronic acid is a strong class of Lewis acid because it has open shell Lewis bases that allow the conversion of sp^2 trigonal hybridization to tetrahedral sp^3 form [1]. It is used as starting material in organic synthesis [3]. In medicine, phenyl boronic acids are used as inhibitors of serine protease and kinase enzymes which increase the growth, progression and metastasis of tumor cells [3–9]. The boron compounds are also used in boron neutron capture therapy of tumors [10, 11]. Likewise, formylphenylboronic acids are important intermediates in the synthesis of active compounds in pharmaceutical industries and are highly effective and important for enzyme stabilizers, inhibitors and bactericides [12]. The addition of various substituents on phenyl rings of boronic acids allows them to be used in a physiologically acceptable pH range and in broader applications [13].

There are many studies on the structural, vibrational and electronic aspects of phenyl boronic acid and its derivatives [14–17]. Zarychta et al. [18] determined the crystal structure of 3-formylphenylboronic acid. Piergies et al. [19] examined 3,4-formyl-substituted phenylboronic acids in terms of structural and vibrational and adsorption modes.

In this study, 3FPBA and 4FPBA molecules were examined both experimentally (FT-IR and dispersive Raman) and theoretically (DFT and TD-DFT) with regard to structural, vibrational, electronical and charge transport properties. The experimental results were consistent with the theoretical results. NBO analysis was performed to explain the charge transfer within the molecules. In addition, electronic properties of 3FPBA and 4FPBA molecules such as UV–Vis spectrum, boundary orbital energies and band gaps were calculated by TD-DFT approach. Anti-apoptotic proteins have important role in the regulation of apoptosis in cancer. Therefore, proteins are consid-

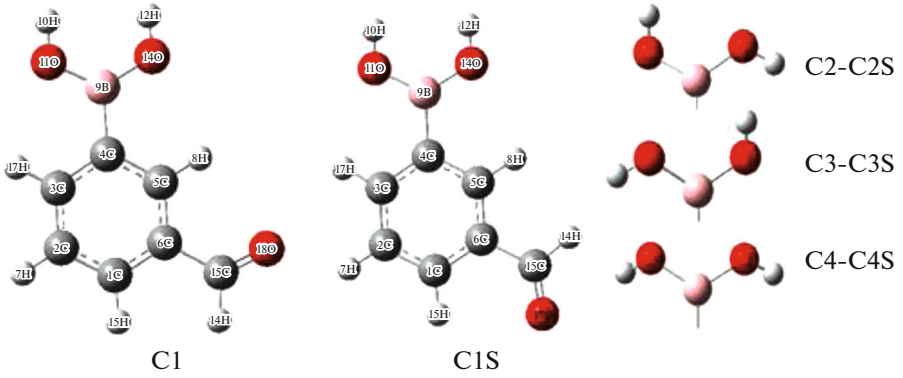

Fig. 1. The optimized structures of 3FPBA for eight possible conformations.

ered as key therapeutic target for cancer treatment. Consequently, our goal was also to design new drug molecule that could potentially bind to anti-apoptotic proteins, thus allowing apoptosis to proceed for cancer therapy.

2. EXPERİMENTAL DETAİLS

The boronic acids 3FPBA and 4FPBA were purchased from Sigma-Aldrich Chemical Company (USA) with a stated purity of 99% (HPLC).

3. COMPUTATİONAL DETAİLS

All calculations for 3FPBA and 4FPBA were made using the Gaussian 09 program package [20] and the results were visualized with the help of the GaussView 5 [21] program. To find the most stable structure of the 3FPBA and 4FPBA molecules, the eight possible conformations were primarily optimized using the DFT/B3LYP/6-311++G(*d*,*p*) [22–24] basis set. Optimized structural parameters are used in vibration frequencies and calculations of electronic properties. The harmonic frequencies were multiplied by the scaling factor [25] to approximate the calculated vibration frequencies to the experimental vibration frequencies. Vibration modes were determined according to VEDA4 program [26]. Many parameters such as UV–Vis spectrum, excitation energies, electronic transitions, absorbance wavelenghts, oscillator strengths were calculated in the ethanol, DMSO and gas phase using the polarizable continuum model (PCM) using the integral equation formalism variant (IEFPCM). Molecular electrostatic potential surface (MEP), Mulliken populations of 3FPBA and 4FPBA compounds were investigated. In addition, NBO analysis and molecular docking were performed for the title compounds. UV–Vis spectra for the studied molecules were calculated using the TD-DFT/B3LYP/6-311+G(*d*,*p*) level of theory. Natural bond orbital (NBO) calculations were performed to understand the intra- and intermolecular bonding of 3FPBA and 4FPBA molecules as well as the interaction between those bonds.

4. RESULTS AND DISCUSSION

4.1. Potential Energy Surface (PES) Scan and Energetics

The reasonable eight conformations of 3FPBA and 4FPBA molecules were analyzed depending on the position of the hydrogen atoms in the $B(OH)_2$ group and the direction of the oxygen atom in the COH group (Figs. 1 and 2).

The energies of these comformations are given in Table 1. For 3FPBA, C3 conformation with −521.75377318 Hartree was calculated as more stable. For 4 FPBA, C3S conformation with −521.75259341 Hartree was calculated as more stable. In addition, all conformations are in C1 symmetry group and have no negative frequency. Structural parameters, vibration frequencies, and UV–Vis spectra of the 3FPBA and 4FPBA molecules were calculated using these most stable structure.

4.2. Structural Analysis

The optimized geometrical structures of the studied compounds are shown in Figs. 3a and 3b. The bond lengths, bond angles and dihedral angles of these structures are given in Table 2, which also shows the crystal data of the phenylboronic acid molecule in the literature [18].

The C–C bond lengths for the phenyl ring of both compounds are almost the same and their values range from 1.39 to 1.43 A and are consistent with the experimental result [18]. The C–H bond lengths on the phenyl ring for 3FPBA are 1.08 A, this length is 1.09 A for 4FPBA, which is greater than the experimental results. These differences result from the intramolecular and non-molecular interaction of 3FPBA and 4FPBA hydrogen bonds. Depending on the substitu-

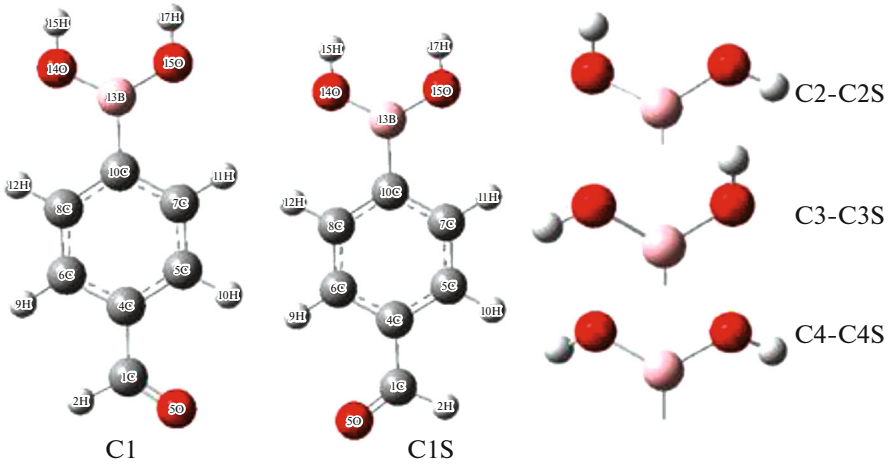

Fig. 2. The optimized structures of 4FPBA for eight possible conformations.

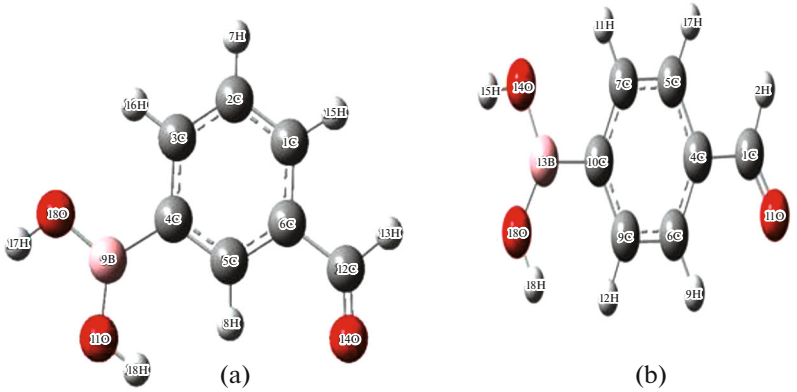

Fig. 3. The optimized structures (a) 3FPBA and (b) 4FPBA.

tion of the COH formyl group for the 3FPBA and 4FPBA molecules, the C–B and C3–C4 bond lengths differ according to each other. Other geometric parameters appear to be in harmony with each other for both molecules, except for small deviations with experimental data.

Table 1. Calculated Energies and energy differences for eight possible conformers of 3FPBA and 4FPBA

Conformers	Energy 3FPBA (Hartree)	Energy differences (Hartree)	Energy 4FPBA (Hartree)	Energy differences (Hartree)
C1	–521.74983613	0.00393705	–521.74976564	0.00282777
C1S	–521.75068596	0.00308722	–521.74976564	0.00282777
C2	–521.75187341	0.00189977	–521.75257616	0.00001725
C2S	–521.75316186	0.00061132	–521.75227596	0.00031745
C3	–521.75377318	0.00000000	–521.75227072	0.00032269
C3S	–521.75295912	0.00081406	–521.75259341	0.00000000
C4	–521.74737972	0.00639346	–521.74701335	0.00558006
C4S	–521.74721509	0.00655809	–521.74563026	0.00696315

Table 2. The some geometrical parameters optimized in 3FPBA and 4FPBA (bond length (Å) and bond angle (deg))

Bond length	Exp. [18]	3FPBA	4FPBA
C1–C2	1.38	1.39	1.39
C1–C6	1.38	1.39	1.40
C1–H15	1.00	1.08	1.09
C2–C3	1.39	1.41	1.40
C2–H7	1.00	1.08	1.09
C3–C4	1.40	1.43	1.41
C3–H16	1.00	1.08	1.09
C4–C5	1.40	1.40	1.39
C4–B9	1.57	1.59	1.57
C5–C6	1.39	1.40	1.40
C5–H8	1.00	1.08	1.09
C6–C12	—	1.54	1.48
B9–O10	1.36	1.35	1.37
B9–O11	1.38	1.38	1.37
O10–H17	0.75	0.96	0.96
O11–H18	0.75	0.96	0.96
C12–H13	—	1.07	1.11
C12–O14	—	1.26	1.21
Bond angle			
C2–C1–C6	120.30	118.81	120.27
C2–C1–H15	120.00	120.60	120.21
C6–C1–H15	120.00	120.60	119.53
C1–C2–C3	120.10	121.56	120.93
C1–C2–H7	120.00	119.54	120.02
C3–C2–H7	120.00	118.90	120.21
C2–C3–C4	121.10	120.30	120.06
C2–C3–H16	120.00	119.85	118.88
C4–C3–H16	120.00	119.85	119.02
C3–C4–C5	117.20	117.65	116.25
C3–C4–B9	122.00	119.89	118.45
C5–C4–B9	–	112.45	111.54
C4–C5–C6	121.80	121.46	120.87
C4–C5–H8	120.00	121.85	120.80
C6–C5–H8	—	116.69	115.45
C1–C6–C5	119.50	119.61	119.45
C1–C6–C12	—	119.75	118.98
C5–C6–C12	—	120.63	119.98
C4–B9–O10	116.30	118.07	118.00
C4–B9–O11	118.70	124.44	123.85
O10–B9–O11	125.00	117.49	117.00
B9–O10–H17	111.00	112.53	112.61
B9–O11–H18	111.00	115.50	115.21
C6–C12–H13	—	114.65	114.57
C6–C12–O14	—	124.89	124.88
H13–C12–O14	—	120.46	120.5
C6–C1–C2–C3	—	0.01	0.36
C6–C1–C2–H7	—	−179.99	−179.73
H15–C1–C2–C3	—	−179.99	−179.75
H15–C1–C2–H7	—	0.0	0.15
C2–C1–C6–C5	—	−0.01	−0.03

4.3. Vibration Spectrum

The measured IR, Raman spectra, and calculated vibrational frequencies and their assignments are listed Table 3.

The experimental and theoretical spectrum are plotted in Figs. 4, 5. The C–H stretching vibrations of the phenyl ring are usually observed in the range of 3100–3000 cm^{-1} [27]. For 3FPBA, these modes are measured at 3218.98 cm^{-1} (IR), 3072.90 cm^{-1} (Raman), they are calculated in the region 3186.59–3147.56 cm^{-1}. The phenyl ring C=C and C–C stretching vibrations normally occur in the range of 1650–1400 cm^{-1} [28]. In the title compounds, C=C and C–C vibrational modes observed in the FT–IR spectrum at 1637, 1619, 1560, 1495, 1410 cm^{-1} (3FPBA) and 1663, 1536, 1406 cm^{-1} (4FPBA) and dis. Raman band at 1672, 1621, 1494 cm^{-1} (3FPBA) and 1670, 1505 cm^{-1} (4FPBA).

The boronic acid vibrational band of the title molecules contain O–H and B–O vibrational modes. The O–H stretching band of boronic acids usually observes 3300–3200 cm^{-1}. Faniran et al. [29] observed the O–H stretching mode at 3280 cm^{-1} for the phenylboronic acid molecule. Tanış et al. [30] reported O–H stretching mode at 3685 and 3692 cm^{-1} for 4-formylphenylboronic acid pinacol ester compound. In this study, FT–IR bands of O–H stretching vibrations for 3FPBA and 4FPBA are calculated 3838, 3872 cm^{-1} and 3838, 3876 cm^{-1}. Sundaraganesan et al. [31] reported the B–O stretching vibration at 1350 cm^{-1} for the phenylboronic acid molecule. Faniran and colleagues [29] observed the B–O stretching mode at 1385 cm^{-1} in the FT–IR spectrum and 1370 cm^{-1} in the FT–Raman spectrum for the 2-fluorophenylboronic acid molecule. For 3FPBA, these modes are obtained at 1393 cm^{-1} (IR), 1397 cm^{-1} (Raman), 1365 and 1382 cm^{-1} (DFT). 4FPBA gives B–O stretching vibrations at 1361 and 1386 cm^{-1} (DFT).

4.4. Mulliken Atomic Charges

The computational atomic charge calculations have an important role in the electronic structure of atomic charges because it affects the dipole moment, molecular polarization capability and many other features of molecular systems [32]. Atomic charges are usually derived from the Mulliken population with some shortcomings [33]. The studied compounds 3FPBA and 4FPBA consist of 18 atoms, The individual atomic charge values obtained from the Muliken population using the DFT/B3LYP/6-311++G(*d*,*p*) basis set are listed in Table 4. All hydrogen and bromine atoms are positively charged because they are atoms acceptor. For 3FPBA, other carbons with the exception of C5 and C6 on the phenyl ring are charged negatively. For 4FPBA, other carbons with the excep-

Table 3. Vibrational assignments of 3FPBA and 4FPBA

Observed frequency (3FPBA)		Calculated frequency (scaled)	Vibrational assigments (%) PED	Observed frequency (4FPBA)		Calculated frequency (scaled)	Vibrational assigments (%) PED
FTIR	FT Raman			FTIR	FT Raman		
		9.46	ΓCCCC(66)			35.62	ΓCCCC(66)
		119.11	ΓBCCC(52)			70.67	ΓBCCC(52)
	121.51	121.16	ΓOCOB(73)		118.27	132.77	ΓOCOB(73)
	166.04	128.03	ΓOBCC(91)		175.97	148.88	ΓOBCC(91)
	211.06	228.36	ΓCCCC(69)			225.78	ΓCCCC(69)
		242.62	ΓCCCC(53)			264.17	ΓCCCC(53)
	333.89	327.01	ΓCCCC(61)			298.82	ΓCCCC(61)
	357.58	404.54	ΓOCCC(80)			409.53	ΓOCCC(80)
		424.84	ΓHCCC(86)			418.54	ΓHCCC(86)
		447.12	ΓHCCC(75)			457.25	ΓHCCC(75)
		448.38	ΓHCCC(85)			465.54	ΓHCCC(85)
		475.23	ΓHCCC(76)			486.02	ΓHCCC(76)
	524.10	533.49	ΓHCCC(67)			571.18	ΓHCCC(67)
	559.56	570.71	ΓHOBC(82)			580.60	ΓHOBC(82)
624.94		661.26	ΓHOBC(92)	638.80	631.52	646.01	ΓHOBC(92)
671.49	686.32	670.56	γBCC(87)	655.27		657.86	γBCC(87)
683.10		713.05	γCCC(77)	704.39	718.56	715.94	γCCC(77)
723.18		713.98	δOBC(78)	732.57		773.49	δOBC(78)
823.94	804.15	814.64	γOBO(82)	825.11	840.65	841.48	γOBO(82)
906.23	906.91	910.82	δCCC(45)			846.83	δCCC(45)
		931.40	γCCC(70)			863.24	γCCC(70)
		953.45	γCCC(60)	962.16		978.66	γCCC(60)
		978.36	δOCC(82)			982.17	δOCC(82)
1047.14		1012.25	δHCO(66)			1000.96	δHCO(66)
		1014.75	γHCC(78)	1013.83		1019.91	γHCC(78)
		1023.24	δHCC(78)			1028.03	δHCC(78)
1078.31		1027.56	γHCC(78)	1036.49		1032.83	γHCC(78)
	1113.36	1104.21	δHCC(78)	1080.20		1114.92	δHOB(78)
1113.57		1125.74	δHOB(68)	1106.95		1127.78	δHCC(68)
1153.05		1190.63	δHOB(69)	1184.96	1171.42	1190.14	δHOB(69)
1216.45	1223.97	1213.73	δCCC(45)	1217.07	1217.73	1229.10	δCCC(45)
1298.91	1267.09	1301.19	νCB(57)	1312.70		1309.20	νCB(57)
1341.22		1346.27	νCC(74)	1341.00		1333.14	νCC(74)
1393.60		1365.09	νOB(65)			1361.84	νOB(65)
	1397.96	1382.21	νOB(54)			1386.08	νOB(54)
1410.62		1414.61	νCC(60)	1406.55		1408.78	νCC(60)
1495.46	1494.19	1457.51	νCC(65)			1437.99	νCC(65)
1560.95		1508.63	νCC(57)	1536.65	1505.76	1533.74	νCC(57)
1619.49	1621.92	1615.02	νCC(55)			1593.72	νCC(55)
1637.67	1672.86	1633.13	νCC(55)	1663.39	1670.51	1643.92	νCC(55)
1738.85		1762.44	νOC(87)	1738.88		1764.63	νOC(87)
2969.98	2883.30	2886.19	νCH(99)	2844.30	2845.02	2886.95	νCH(99)
	3072.17	3147.56	νCH(99)	638.80	3067.57	3132.25	νCH(99)
		3152.62	νCH(99)	655.27		3152.57	νCH(99)
		3171.81	νCH(99)	3200.69		3184.56	νCH(99)
3218.98		3186.59	νCH(96)			3185.93	νCH(96)
		3838.41	νOH(100)			3838.62	νOH(100)
		3872.26	νOH(100)			3876.88	νOH(100)

ν is stretching, δ is in plane bending, γ is out of plane bending, Γ is torsion, ρ is scissoring.

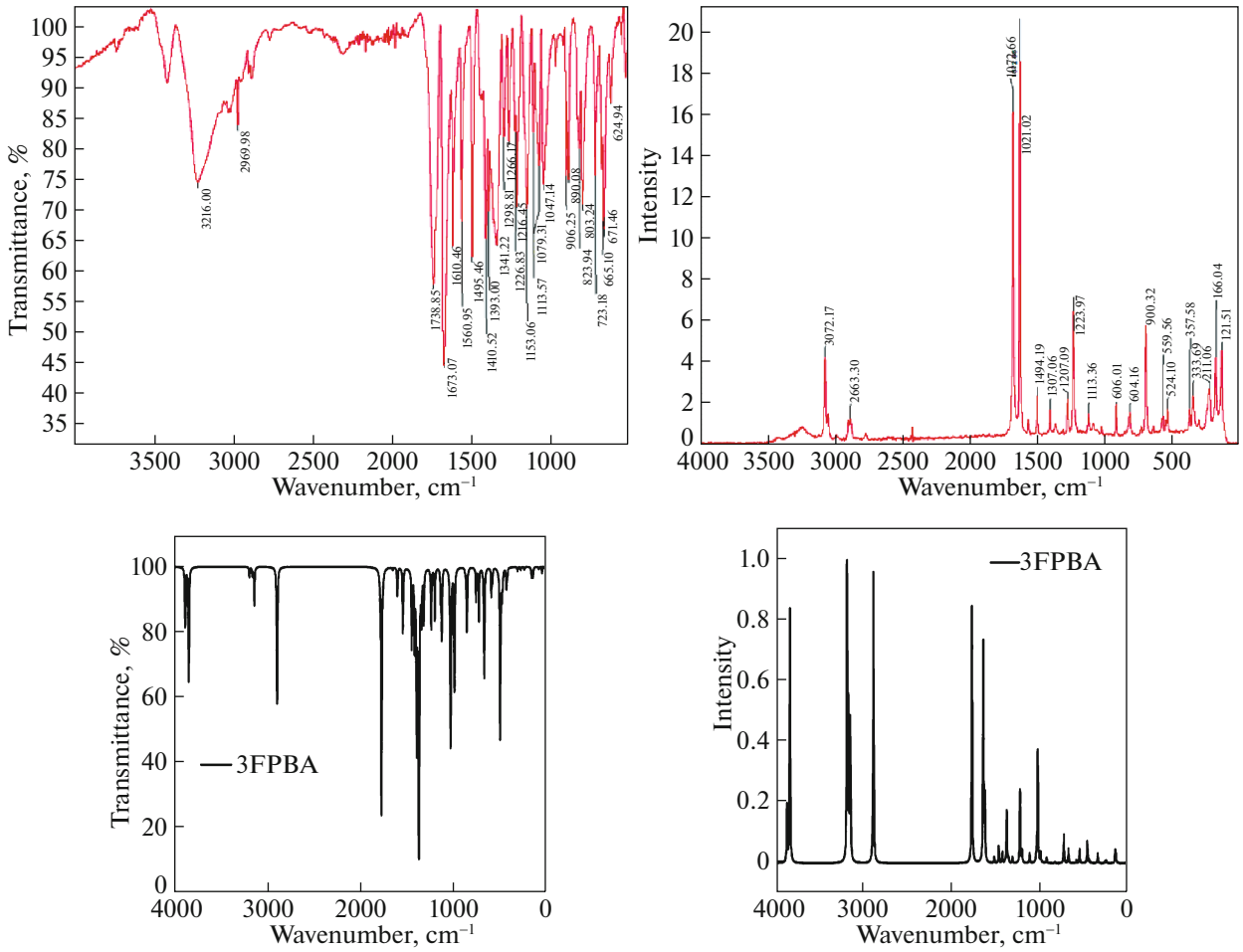

Fig. 4. The experimental FT–IR and dis. Raman spectra of 3FPBA.

tion of C4 and C6 on the phenyl ring are charged negatively. The C atoms (3FPBA/C6, 4FPBA/C4) with the origin of the formula group for each compound are very high. For both compounds, the Mulliken charges of the C atoms (3FPBA/C6, 4FPBA/C4) linked to the formula group (C=OH) are very high. For both molecules, the atoms of the formyl groups and the boronic acid groups have almost the same charge values.

4.5. NBO Analysis

In computational chemistry, the natural bond orbital is used to calculate the distribution of bonds, donor–acceptor interactions and electron density between atoms, depending on the density of electrons. NBO calculations of the 3FPBA and 4FPBA were obtained as implemented in Gaussian 09 program and the results are reported in Tables 5 and 6. The magnitude of $E(2)$ indicates the power of interaction between electron donors and electron acceptors, the tendency to give more electrons from electron donors to electron receptors, and the level of conjugation of the whole system. Some intramolecular hyperconjugative interactions in 3FPBA are $\pi C1-C6 \rightarrow \pi^*C2-C3$, $\pi C1-C6 \rightarrow \pi^*C4-C5$, $\pi C2-C3 \rightarrow \pi^*C1-C6$ with stabilization energies 68.53, 86.15, 100.00 kcal/mol. The similar interactions are calculated in 4FPBA with completely different energies, they are $\pi C4-C5 \rightarrow \pi^*C1-O3$, $\pi C7-C10 \rightarrow \pi^*C4-C5$, $\pi C7-C8 \rightarrow \pi^*C6-C8$ with stabilization energies 19.43, 21.84, 18.81 kcal/mol. The stabilization energies clear that the orbital interactions in 3FPBA are much stronger than 4FPBA.

4.6. Electronic Properties

4.6.1. Molecular electrostatic potential surface. The molecular electrostatic potential (MEP) surface map is an electrostatic potential graph on the surface of the constant electron density [34]. The molecular MEP surface diagrams are useful in understanding the physicochemical structure of a molecule since it shows the molecular properties like the size and shape as well as the regions with positive, negative and neutral electrostatic potential depending on color grading

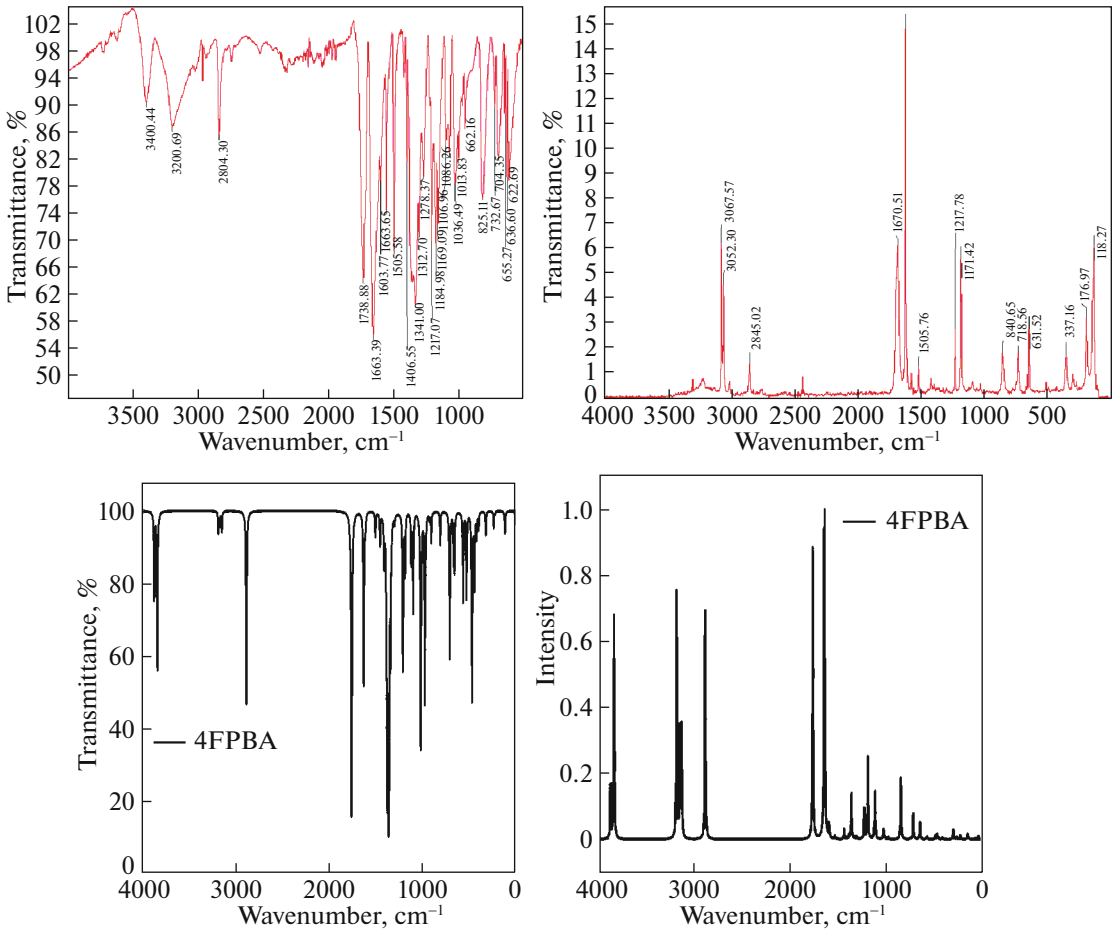

Fig. 5. The experimental FT–IR and dis. Raman spectra of 4FPBA.

[35, 36]. It is a calculation technique frequently used to work out the nucleo- and electrophilic attacks in molecules.

At this visual presentation of chemical activity, the negative (red) regions of MEP are related to electrophilic reactivity and electron–donating reaction while the positive (blue) regions are pertinent to nucleophilic reactivity and electron–accepting reaction. MEP maps for the title compounds were performed using the basis set of B3LYP/6-311++G(*d*,*p*) and presented in Fig. 6. All colors in this range from red to blue were used. Different colors on the MEP surface map show different values of electrostatic potential. The MEP surfaces are displayed by color coding in the range from –5.680 a.u. (deepest red) to 5.680 a.u. (deepest blue) for 3FPBA and –6.675 to 6.675 a.u. for 4FPBA, which 3FPBA has a stronger positive and negative charge distribution compared to 4FPBA.

4.6.2. Frontier molecular orbitals. The lowest empty orbital (LUMO) known to the ability to receive electrons with the highest full orbital (HOMO) known to the ability to give electrons is important orbital. Because the difference between E_{HOMO} and E_{LUMO} can explain the electrical and optical parameters of the molecule, its chemical reactivity and its stability [37, 38]. The frontier molecular orbitals (HOMO and LUMO) energy was calculated by TD–DFT/B3LYP/6-311++G(*d*,*p*) method in DMSO, ethanol solutions and gas phase. The HOMO–LUMO shapes of the title molecules in the gas phase are given in Fig. 7. Red and green colors indicate the positive and negative phases of the molecular orbital, respectively. HOMO orbital was localized except for the B (OH) group in both the 3FPBA and 4FPBA molecules. The LUMO orbital was localized except for B(OH) group for 3FPBA, but localized on the whole molecule for the 4FPBA molecule. The energy gap (E_g) which is the energy difference between HOMO and LUMO orbital is a critical parameter in measuring the electron conductivity and molecular reactivity. This value calculated as 5.35 eV for 3FPBA and 4.96 eV for 4FPBA in the gas phase. Also, a molecule with small frontier orbital gap is named as a soft molecule. Soft molecules are more polarizable and have a high

Table 4. Mulliken atomic charges for 3FPBA and 4FPBA performed at B3LYP method with 6-311++G(*d*,*p*) basis set

Atom (3FPBA)	Mulliken charges (a.u.)	Atom (4FPBA)	Mulliken charges (a.u.)
C1	–0.774	C1	–0.135
C2	–0.292	H2	0.135
C3	–0.005	O3	–0.236
C4	–0.754	C4	0.757
C5	0.056	C5	–0.839
C6	1.044	C6	0.246
H7	0.185	C7	–0.135
H8	0.182	C8	–0.252
B9	0.546	H9	0.198
O10	–0.367	C10	–0.508
011	–0.352	H11	0.196
C12	–0.199	H12	0.132
H13	0.130	B13	0.507
O14	–0.238	O14	–0.364
H15	0.144	H15	0.285
H16	0.181	O16	–0.342
H17	0.278	H17	0.164
H18	0.236	H18	0.240

chemical reactivity as well as low kinetic stability [39]. Therefore, it can be said that the reactivity and softness of the 4FPBA is better than the 3FPBA.

4.6.3. UV–Vis spectra. Interaction of light with molecules is important to understand its electronic and optic structure. The molecular electronic absorption wavelength (λ), excitation energies (*E*), oscillator strengths (*f*), and major contribution of assignments electronic transitions were calculated using the method/basis set TD–DFT–B3LYP/6-311++G (*d*,*p*) in ethanol, DMSO and gas phase in Table 7. From the table it is seen that the electronic transition from the ground state to the first excited state is from HOMO (39) to LUMO (40). This transition also defines the maximum absorption that have the highest oscillator strength at the same time. The lowest excitation energy for electronically transition from the ground state to the excited state is 3.69 eV for 3FPBA and 3.55 eV for 4FPBA.

4.7. Molecular Docking

Docking results were obtained from two different programs; Autodock Vina and VMD (version 1.9.3) [40, 41]. The binding strength was defined by use of scoring function based on the Lamarckian Genetic Algorithm. The highest binding score represents tight binding between the protein and ligand. In our study the highest binding score were obtained between 3FPBA and 4FPBA molecule and antiapoptotic protein BRAF, 6.8 and –6.5 kcal/mol, respectively. The docking results calculated by the Vina software for 3FPBA–BCL-2, 3FPBA–BCL-w, 3FPBA–MCL-1 and 4FPBA–BCL-2, 4FPBA–BCL-w, 4FPBA–MCL-1 complexes were, –5.8, –6.2, –6.3, –5.7, –6.3, and –6.1 kcal/mol, respectively (Table 8 and Figs. 8S–15S (Supplementary Materials)).

5. CONCLUSİONS

The structures of the title compounds were examined in detail using computational chemistry. The optimized structural parameters and vibrational

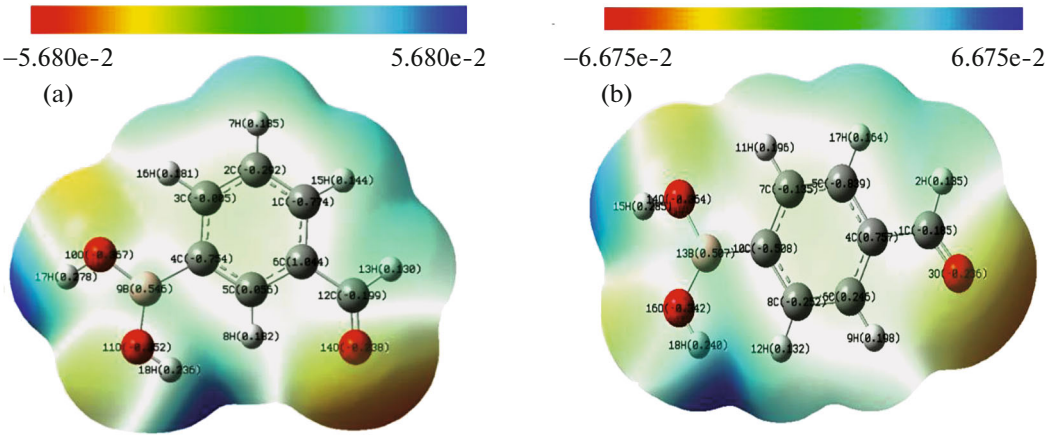

Fig. 6. Molecular electrostatic potential surfaces of (a) 3FPBA and (b) 4FPBA.

Table 5. Second order perturbation theory analysis of Fock matrix in NBO basis for 3FPBA

Donor (*i*)	Type	ED/e	Acceptor (*j*)	Type	ED/e	$E^{(2)}$, kJ mol^{-1}	$E(j) - E(i)$, a.u.	$F(i,j)$, a.u.
C1–C2	σ	1.97	C1–C6	σ*	0.02	12.68	1.27	0.055
C1–C2	σ	1.97	C2–C3	σ*	0.01	11.51	1.29	0.053
C1–C2	σ	1.97	C6–C12	σ*	0.05	13.85	1.15	0.056
C1–C6	σ	1.97	C1–C2	σ*	0.01	11.30	1.28	0.053
C1–C6	σ	1.97	C1–C2	σ*	0.01	11.30	1.28	0.053
C1–C6	σ	1.97	C5–C6	σ*	0.02	17.28	1.28	0.065
C1–C6	π	1.63	C2–C3	π*	0.01	68.53	0.29	0.063
C1–C6	π	1.63	C4–C5	π*	0.02	86.15	0.29	0.070
C1–C6	π	1.63	C12–O14	π*	0.01	84.73	0.27	0.071
C1–H15	σ	1.97	C2–C3	σ*	0.01	15.10	1.11	0.057
C1–H15	σ	1.97	C5–C6	σ*	0.02	19.71	1.10	0.064
C2–C3	σ	1.98	C3–C4	σ*	0.02	11.76	1.27	0.053
C2–C3	π	1.64	C1–C6	π*	0.36	100.00	0.28	0.073
C2–C3	π	1.64	C4–C5	π*	0.29	69.37	0.29	0.063
C2–H7	σ	1.98	C1–C6	σ*	0.36	14.81	1.09	0.055
C2–H7	σ	1.98	C3–C4	σ*	0.02	16.36	1.09	0.058
C3–C4	σ	1.97	C4–C5	σ*	0.02	15.40	1.28	0.061
C3–C4	σ	1.97	C5–H8	σ*	0.01	13.14	1.13	0.053
C3–H16	σ	1.97	C1–C2	σ*	0.01	16.65	1.09	0.059
C3–H16	σ	1.97	C4–C5	σ*	0.02	18.41	1.10	0.062
C4–C5	π	1.97	B9	LP*(1)	0.36	90.33	0.27	0.068
C4–C5	π	1.97	C1–C6	π*	0.36	79.24	0.28	0.065
C4–C5	π		C2–C3	π*	0.28	88.74	0.28	0.070
C12–O14	π	1.98	C1–C6	π*	0.39	20.42	0.40	0.044
B9	LP*(1)	1.99	C4–C5	π*	0.29	491.20	0.02	0.075
O10	LP (2)	1.99	B9	LP*(1)	0.36	222.97	0.33	0.124
O11	LP(2)	1.99	B9	LP*(1)	0.36	217.23	0.33	0.124
O14	LP(2)	1.99	C6–C12	σ*	0.05	73.39	0.71	0.101
O14	LP(2)	1.99	C12–H13	σ*	0.06	96.23	0.62	0.108
C1–C6	π*	1.62	C4–C5	π*	0.29	1149.93	0.01	0.082

Table 6. Second order perturbation theory analysis of Fock matrix in NBO basis for 4FPBA

Donor (*i*)	Type	ED/e	Acceptor(*j*)	Type	ED/e	$E^{(2)}$, kJ mol^{-1}	$E(j) - E(i)$, a.u.	$F(i,j)$, a.u.
C1–H2	σ	1.98	C4–C6	σ*	0.02	4.10	1.10	0.060
C1–O3	σ	1.99	C1–C4	σ*	0.05	1.03	1.52	0.036
C1–O3	π	1.97	C4–C5	Π*	0.36	5.00	0.41	0.044
C1–C4	σ	1.98	C4–C5	σ*	0.02	1.88	1.24	0.043
C1–C4	σ	1.98	C5–C7	σ*	0.01	2.32	1.25	0.048
C1–C4	σ	1.98	C6 –C8	σ*	0.01	2.31	1.25	0.048
C4–C5	σ	1.97	C4–C6	σ*	0.02	3.89	1.27	0.063
C4–C5	σ	1.97	C5–C7	σ*	0.01	2.84	1.29	0.054
C4–C5	π	1.62	C1–O3	π*	0.10	19.43	0.27	0.070
C4–C5	π	1.62	C6–C8	π*	0.01	19.05	0.29	0.068
C4–C5	π	1.62	C7–C10	π*	0.32	19.13	0.29	0.067
C4–C6	σ	1.97	C4–C5	σ*	0.02	3.89	1.27	0.063
C5–C7	σ	1.98	C1–C4	σ*	0.05	3.24	1.15	0.055
C5–H17	σ	1.97	C4–C6	σ*	0.02	4.60	1.09	0.063
C6–C8	σ	1.98	C8–C10	σ*	0.02	3.25	1.28	0.057
C6–C8	π	1.65	C4–C5	π*	0.36	19.52	0.28	0.067
C6–C8	π	1.65	C7–C10	π*	0.32	19.90	0.29	0.068
C6–H9	σ	1.97	C4–C5	σ*	0.02	4.63	1.09	0.063
C6–H9	σ	1.97	C8–C10	σ*	0.02	4.05	1.08	0.059
C7–C10	π	1.61	B13	LP*(1)	0.36	21.09	0.26	0.066
C7–C10	π	1.61	C4–C5	π*	0.36	21.84	0.27	0.069
C7–C10	π	1.61	C6–C8	π*	0.27	18.81	0.28	0.066
C7–H11	σ	1.97	C8–C10	σ*	0.02	4.38	1.08	0.061
C8–H12	σ	1.98	C7–C10	σ*	0.02	4.05	1.10	0.060
C10–B13	σ	1.96	C5–C7	σ*	0.01	4.14	1.12	0.061
C10–B13	σ	1.96	C6–C8	σ*	0.01	4.14	1.12	0.061
O3	LP(2)	1.87	C1–H2	σ*	0.06	23.07	0.62	0.108
O3	LP(2)	1.87	C1–C4	σ*	0.05	17.70	0.71	0.102
B13	LP*(1)	0.36	C7–C10	π*	0.32	110.67	0.02	0.076
O14	LP(2)	1.83	B13	LP*(1)	0.36	53.69	0.33	0.124
O16	LP(2)	1.83	B13	LP*(1)	0.36	51.49	0.33	0.123
C1–O3	π*	0.10	C4–C5	π*	1.62	135.83	0.01	0.070

Table 7. The calculated wavelengths λ (nm), excitation energies (eV), oscillator strengths (*f*) of 3FPBA and 4FPBA in ethanol, DMSO, and gas phase

3FPBA				4FPBA			
energy, eV	wavelength, nm	osc. strength	major contributions	energy, eV	wavelength, nm	osc. strength	major contributions
Gas phase							
3.69	336.17	0.0001	39–40	3.55	349.35	0.0001	39–40
4.62	268.58	0.0098	37–40 38–40	4.48	276.76	0.0272	37–40 38–40 38–41
5.10	243.01	0.0001	39–41	4.93	251.41	0.3766	37–40 38–41
DMSO							
3.81	325.34	0.0001	38–40	3.70	335.40	0.0001	38–40 38–43
4.53	273.45	0.0205	39–40	4.37	283.72	0.0392	37–40 37–41 39–40
4.95	250.30	0.2918	37–40 39–40 39–41	4.79	258.66	0.4947	37–40
Ethanol							
3.81	325.61	0.0001	38–40	3.69	335.77	0.0001	38–40 39–43
4.54	273.26	0.0195	37–40 37–41 39–41	4.37	283.39	0.0378	37–40 37–41 39–40
4.96	249.85	0.2823	37–40 39–40 39–41	4.80	258.09	0.4834	37–40

spectra analysis of title molecules have been obtained at DFT/B3LYP/6-311++G(*d*,*p*) level. Theoretically calculated geometric parameters and frequencies show good correlation with the experimental values. The excitation energy of the 3FPBA molecule in both the solvent and the gas phase was calculated to be higher than that of 4FPBA molecule. Energy gap values between HOMO and LUMO orbitals of 4FPBA molecule is less than that for 3FPBA molecule, this indicates that 4FPBA is more reactive than 3FPBA. The stabilization energies show that the orbital interactions in 3FPBA are much stronger than 4FPBA. In the present study, we have designed and analyzed a 3FPBA and 4FPBA in order to obtain new drug active molecules. The aforementioned investigation has not been reported in the literature so far. So this study shows that the molecular interaction affinities between antiapoptotic targets and compounds based on molecular docking. The obtained molecular docking results will aid in better understanding of its molecular interaction with antiapoptotic proteins.

Table 8. Docking binding energy results of 3FPBA and 4FPBA molecule as inhibitor with antiapoptotic proteins

3FPBA	Binding energy, kcal/mol
BRAF	–6.8
BCL-2	–5.8
BCL-w	–6.2
Mcl-1	–6.3
4FPBA	Binding energy, kcal/mol
BRAF	–6.5
BCL-2	–5.7
BCL-w	–6.3
Mcl-1	–6.1

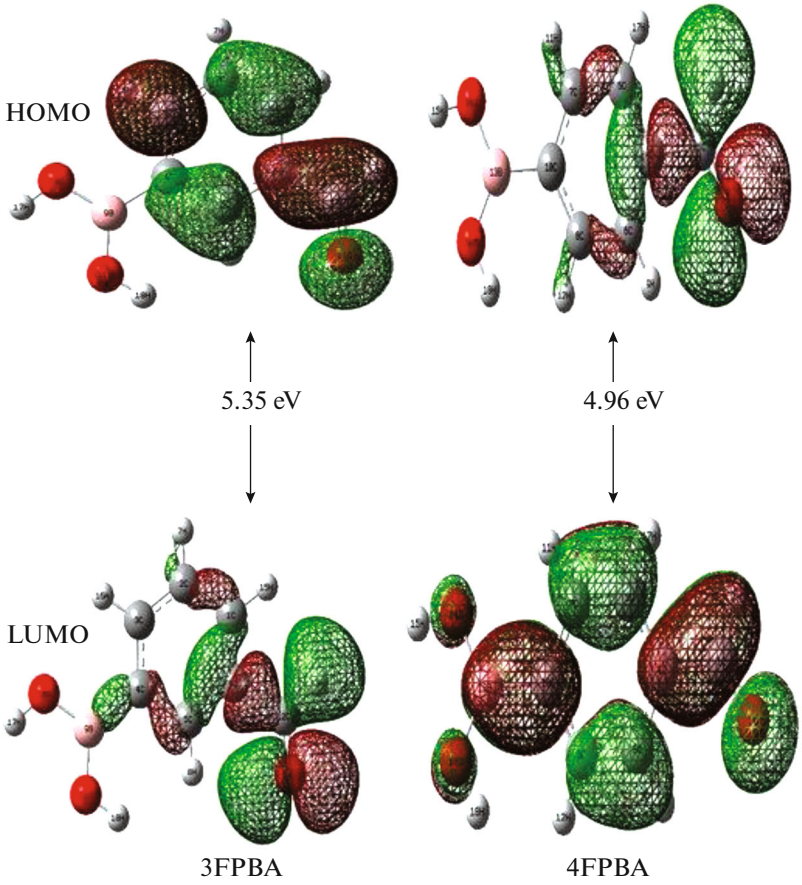

Fig. 7. Highest occupied and lowest unoccupied molecular orbitals of 3FPBA and 4FPBA calculated at B3LYP/6-311++G(*d*,*p*) level.

ACKNOWLEDGMENTS

The numerical calculations were performed at TUBITAK ULAKBIM, High Performance and Grid Computing Center and Kırşehir Ahi Evran University, Research and Application Center. We are thankful to TUBITAK and Kırşehir Ahi Evran University.

SUPPLEMENTARY MATERIALS

Supplementary materials are available for this article at https://doi.org/10.1134/S0036024420130282 and are accessible for authorized users.

REFERENCES

1. N. A. Petasis, Aust. J. Chem. **60**, 795 (2007).
2. P. C. Trippier and C. McGuigan, Med. Chem. Commun. **1**, 183 (2010).
3. W. Yang, X. Gao, and B. Wang, Med. Res. Rev. **23**, 346 (2003).
4. J. Zhang, P. L. Yang, and N. S. Gray, Cancer **9**, 28 (2009).
5. C. Tsatsanis and D. A. Spandidos, Int. J. Mol. Med. **5**, 583 (2000).
6. N. M. Giles, G. I. Giles, and C. Jacob, Biochem. Biophys. Res. Commun. **300**, 1 (2003).
7. C. J. Watson and P. A. Kreuzaler, J. Mamm. Gland Biol. Neoplas. **14**, 171 (2009).
8. E. Tsilikounas, C. A. Kettner, and W. Bachovchin, Biochemistry **31**, 12839 (1992).
9. T. Asano, H. Nakamura, Y. Uehara, and Y. Yamamoto, ChemBioChem. **5**, 483 (2004).
10. A. H. Soloway, W. Tjarks, B. A. Barnum, F. G. Rong, R. F. Barth, I. M. Codogni, and J. G. Wilson, Chem. Rev. **98**, 1515 (1998).
11. D. H. Kinder, S. K. Frank, and M. M. Ames, J. Med. Chem. **33**, 819 (1990).
12. H. Suenaga, K. Nakashima, M. Mikami, H. Yamamoto, T. D. James, K. R. Sandanayake, and A. S. Shinkai, Recl. Trav. Chim. Pay-Bas. **115**, 44 (1996).
13. L. Santuci and H. Gilman, J. Am. Chem. Soc. **80**, 193 (1958).
14. J. A. Faniran and H. F. Shurvell, Can. J. Chem. **46**, 2089 (1968).
15. M. Kurt, J. Ram. Spect. **40**, 67 (2009).
16. M. Kurt, J. Mol. Struct. **874**, 159 (2008).
17. S. Fereidoni, R. Ghiasi, H. Pasdar, and B. Mohtat, J. Struct. Chem. **60**, 1743 (2019).

18. B. Zarychta, J. Zaleski, A. Sporzynski, M. Dabrowski, and J. Serwatowski, Acta Crystallogr., C **60**, o344 (2004).
19. N. Piergies, E. Proniewicz, Y. Ozaki, Y. Kim, and L. M. Proniewicz, J. Phys. Chem. A **117**, 5693 (2013).
20. M. J. Frisch et al., *Gaussian 09, Revision A.1* (Gaussian Inc., Wallingford, CT, 2009).
21. E. Frisch, H. P. Hratchian, R. D. Dennington II, T. A. Keith, J. Millam, B. Nielsen, A. J. Holder, and J. Hiscocks, *GaussView, Version 5.0.8* (Gaussian, Inc., Wallingford, CT, 2009).
22. P. Hohenberg and W. Kohn, Phys. Rev. B **136**, 864 (1964).
23. A. D. Becke, J. Chem. Phys. **98**, 5648 (1993).
24. C. Lee, W. Yang, and R. G. Parr, Phys. Rev. B **37**, 785 (1988).
25. H. Watanabe, N. Hayazawa, Y. Inouye, and S. Kawata, J. Phys. Chem. B **109**, 5012 (2005).
26. M. H. Jamroz, *Vibrational Energy Distribution Analysis VEDA 4* (Warsaw, Poland, 2004).
27. J. Coates, in *Encyclopedia of Analytical Chemistry,* Ed. by R. A. Meyers (Wiley, Chichester, 2000).
28. G. Varsanyi, *Assignments for Vibrational Spectra of Seven Hundred Benzene Derivatives* (Adam Hilger, London, 1974), Vols. 1–2.
29. J. A. Faniran and H. F. Shurvell, Can. J. Chem. **46**, 2089 (1968).
30. E. Tanış, E. B. Şaş, M. Kurban, and M. Kurt, J. Mol. Struct. **1154**, 301 (2018).
31. N. Sundaraganesan, S. Ilakiamani, H. Salem, P. M. Wojciechowski, and D. Michalska, Spectrochim. Acta, A **61**, 2995 (2005).
32. E. R. Davidson and S. X. Chakravarthy, Theor. Chim. Acta **83**, 319 (1992).
33. P. Hohenberg and W. Kohn, Phys. Rev. B **136**, 864 (1964).
34. K. Vanasundari, V. Balachandran, M. Kavimani, and B. Narayana, J. Mol. Struct. **1155**, 21 (2018).
35. J. Murray and K. Sen, *Molecular Electrostatic Potentials: Concepts and Applications,* 1st ed. (Elsevier, Amsterdam, 1996).
36. E. Scrocco and J. Tomasi, Adv. Quantum Chem. **11**, 115 (1978).
37. A. D. Jenkins, R. G. Jones, and G. Moad, Pure Appl. Chem. **82**, 483 (2010).
38. I. Fleming, *Frontorbitale: Frontier Orbitals and Organic Chemical Reactions* (Wiley, New York, 1976).
39. R. S. Mulliken, J. Chem. Phys. **2**, 782 (1934).
40. W. Humphrey, A. Dalke, and K. Schulten, J. Mol. Graph. **14**, 33 (1996).
41. O. Trott and A. J. Olson, J. Comput. Chem. **31**, 455 (2010).